JACS
JOURNAL OF THE AMERICAN CHEMICAL SOCIETY
pubs.acs.org/JACS
Article

Calix[4]pyrrolato-germane-$(thf)_2$: Unlocking the Anti-van't Hoff–Le Bel Reactivity of Germanium(IV) by Ligand Dissociation

Ravi Yadav,[‡] Paul Janßen,[‡] Marcel Schorpp, and Lutz Greb*

Cite This: *J. Am. Chem. Soc.* 2023, 145, 17746–17754
Read Online
ACCESS | Metrics & More | Article Recommendations | Supporting Information

ABSTRACT: Anti-van't Hoff–Le Bel configured p-block element species possess intrinsically high reactivity and are thus challenging to isolate. Consequently, numerous elements in this configuration, including square-planar germanium(IV), remain unexplored. Herein, we follow a concept to reach anti-van't Hoff–Le Bel reactivity by ligand dissociation from a rigid calix[4]pyrrole germane in its bis(thf) adduct. While the macrocyclic ligand assures square-planar coordination in the uncomplexed form, the labile thf donors provide robustness for isolation on a multigram scale. Unique properties of a low-lying acceptor orbital imparted to germanium(IV) can be verified, e.g., by isolating an elusive anionic hydrido germanate and exploiting it for challenging bond activations. Aldehydes, water, alcohol, and a CN triple bond are activated for the first time by germanium-ligand cooperativity. Unexpected behaviors against fluoride ion donors disclose critical interferences of a putative redox-coupled fluoride ion transfer during the experimental determination of Lewis acidity. Overall, we showcase how ligand lability grants access to the uncharted chemistry of anti-van't Hoff–Le Bel germanium(IV) and line up this element as a member in the emerging class of structurally constrained p-block elements.

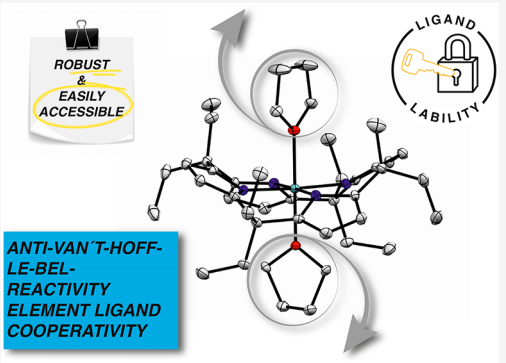

INTRODUCTION

The chemistry of p-block element compounds as a key driver for bond activation reactions and their use as catalysts is a highly active field of research.[1] Besides the established strategies to enhance the reactivity of p-block elements by low oxidation[2] or valence states,[3] manipulation of frontier molecular orbital (FMO) energies by structural constraint approaches is gaining recent interest.[4] Accordingly, p-block compounds in non-VSEPR geometries enabled an array of reactivities previously restricted to transition metals or low-valent p-block compounds (refs 1–6). While most achievements in this area are based on the deformation of group 13[4h,5] and 15[1e,4g,i,6] elements (see Figure 1A for selected examples), only a few structurally constrained group 14 elements have been reported.[7] However, based on the predicted changes in frontier molecular orbital energies, the induced effect should be most pronounced upon the planarization of tetrahedral group 14 species.[8] A square planar germanium corrole cation $[TPFC\text{-}Ge][B(C_6F_5)_4]$ (TPFC = tris(pentafluorophenyl)-corrole) (Figure 1B) turned out as highly reactive, rendering solid-state isolation and characterization as unsuccessful.[9] Despite our recent success in isolating the first square planar coordinated silicon(IV) species, its broader application also remains hindered by a straightforward, large-scale synthesis and its thermal instability, highlighting the remaining challenges in this field. Hence, we reasoned if anti-van't Hoff–Le Bel reactivity could be reached by combining a structurally constraining, macrocyclic ligand with additional labile ligands that are deliberated before substrate activation (Figure 1C). This approach would allow unlocking and gauging anti-van't Hoff–Le Bel reactivity while maintaining robust starting materials and conditions. Herein, the multigram scale synthesis, characterization, and reactivity of donor stabilized calix[4]pyrrolato-germane, $[CxGe(thf)_2]$ **1** (Cx = *meso*-octaethylcalix[4]pyrrolato) is reported (Figure 2A). The putative donor-free CxGe features a square-planar global minimum and a germanium-centered LUMO with an even smaller FMO-gap (3.17 eV) compared to the isolated silicon derivative CxSi (3.44 eV; see section 4.7 in the Supporting Information (SI)). The observed reactivity outlines how ligand dissociation from an unprecedented neutral anti-van't Hoff–Le Bel germanium(IV) leverages reaction modes not observed priorly for this element. Complex **1** is hydrocarbon soluble and opens multimodal reactivity patterns, including access to the first anionic hydrido germanate and element-ligand cooperative (ELC) activation of single and multiple bonds. The Lewis acid **1** abstracts fluoride from $[SbF_6]^-$, while $[PF_6]^-$ remains untouched. This anomaly indicates an electron-coupled

Received: April 28, 2023
Published: August 7, 2023

https://doi.org/10.1021/jacs.3c04424
J. Am. Chem. Soc. 2023, 145, 17746–17754

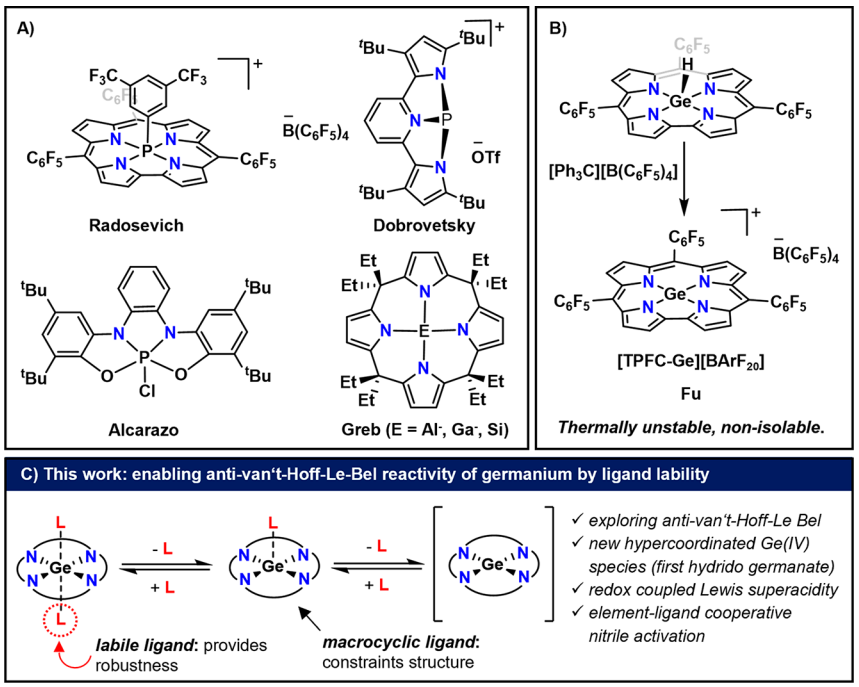

Figure 1. (A) Examples of structurally constrained p-block complexes, mainly limited to group 15. (B) *In-situ* generation of 4-coordinate square planar germanium(IV) cation [TPFC-Ge]. (C) Concept followed in this work.

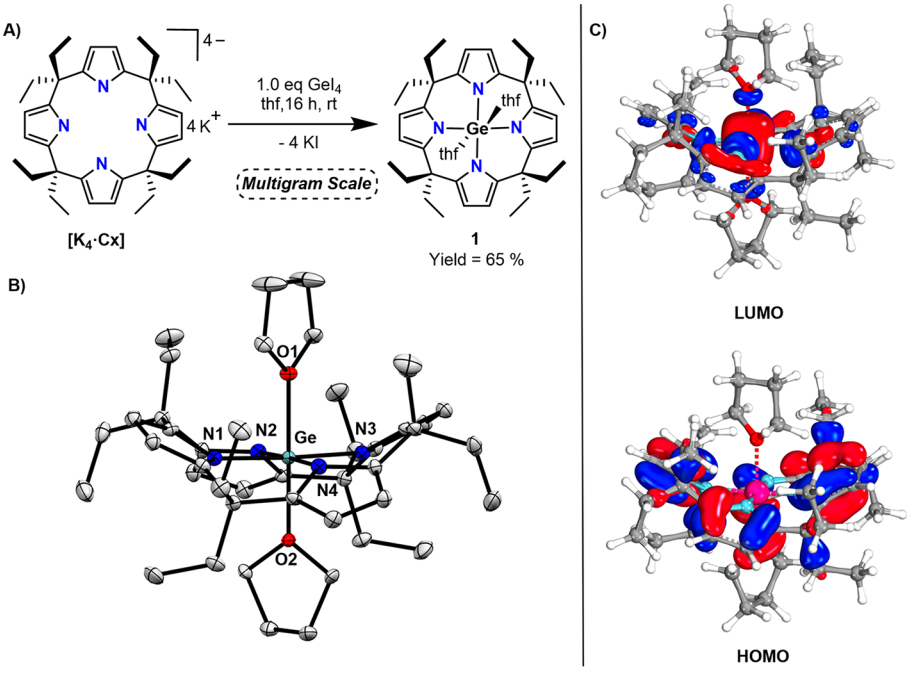

Figure 2. (A) Synthesis of **1**. (B) Solid state structure of **1**, displacement ellipsoids are drawn at 50% probability level, and hydrogen atoms are omitted for clarity. Selected bond lengths (pm) and angles (deg): $d_{\varnothing}$(Ge−N) 196.5(34), $d_{\varnothing}$(Ge−O) 205.1(27), N1−Ge−N4 177.9(11), N2−Ge−N3 176.7(11). (C) Frontier molecular orbitals of **1** calculated at the PW6B95-D3(BJ)/def2-QZVPP//r^{2}scan-3c level of theory.

fluoride ion transfer and urges caution for the experimental evaluation of Lewis superacidity with redox-active Lewis acids.

RESULTS AND DISCUSSION

Initially we attempted the synthesis of a square planar germane by reacting the potassium salt of the octaethylcalix[4]pyrrole [K_4·Cx][7b] with GeI_4 in noncoordinating solvents such as dcm and *o*-difluorobenzene. In the absence of coordinating solvent, the byproduct KI reacts further, resulting in the formation of KCxGeI. The separation of residual KI and KCxGeI was tedious, and this route was not followed further. The reaction of [K_4·Cx][7b] with GeI_4 in thf resulted in the formation of [CxGe(thf)$_2$] (**1**) in an isolated yield of 65% at a multigram scale (Figure 2A). The identity and purity of **1** are established in solution and in the solid state by NMR and elemental analysis. The ^{1}H NMR spectrum of complex **1** in benzene-d_6 or dcm-d_2 shows one singlet for the pyrrolic protons and a single set of signals for the ethyl protons, in line with a pseudo-

https://doi.org/10.1021/jacs.3c04424
J. Am. Chem. Soc. 2023, 145, 17746−17754

D_{4h} symmetric species in solution. Interestingly, all signals are broadened, which is attributed to the dynamic coordination of thf and the coupled ring inversion of the calix[4]pyrrole macrocycle. A solution of **1** in CD_2Cl_2 in the presence of 5 equiv of thf shows only one set of signals for both the Ge-bound and free thf molecules, corroborating the labile binding of the thf molecules (Figure S4). Single crystal X-ray diffraction (SCXRD) studies of complex **1** revealed an octahedral coordinated germanium atom with a planar [N_4Ge] motif, with the Ge atom further coordinated by two oxygen atoms of thf in the *trans* position (Figure 2B). Compound **1** represents the first example of calix[4]pyrrole complex of germanium.[10] The Ge−$N_{average}$ bond distance (197.50(2) pm) is elongated as compared to [(TPFC)Ge-(thf)$_2$]$^+$ (Ge−$N_{average}$ = 189.6(2) pm), which can be attributed to the larger cavity size of **1** (7727 pm^2) versus [(TPFC)Ge-(thf)$_2$]$^+$ (7161 pm^2),[11] and the cationic charge in the latter.[9a] The Ge−$O_{average}$ bond distance in **1** (205.1(2) pm) is slightly shorter than that in [(TPFC)Ge(thf)$_2$]$^+$ (206.8(4) pm).[9a]

Having experimentally accessed the desired compound, some properties were assessed by density functional theory. The highest occupied molecular orbital (HOMO) of **1** is delocalized across the ligand backbone, while the lowest unoccupied molecular orbital (LUMO) remains located at the germanium level (Figure 2C). This scenario indicates a Ge-centered Lewis acidity and is desirable for ambiphilic, element-ligand cooperative reactivity.[10] Moreover, calix[4]pyrrolato complexes with ligand-centered HOMO are known to act as efficient two- and four-electron transfer reagents, an aspect that becomes of importance during fluoride abstraction reactivity (*vide infra*).[6a,12] The binding enthalpy for the first THF from **1** to a square pyramidal germane is computed to $\Delta H_{(dcm)}$ = −17.9 kcal mol^{-1} ($\Delta G_{(dcm)}$ = −5.9 kcal mol^{-1}) (DSD-PBEP86-D3(BJ)/def2-QZVPP+COSMO-RS(DCM)//r^{2}SCAN-3c), thus in line with the observed dynamics in CH_2Cl_2 solution. The binding enthalpy of the second thf was computed to be $\Delta H_{(dcm)}$ = −23.9 kcal mol^{-1} ($\Delta G_{(dcm)}$ = −13.0 kcal). The thf-free compound features a global minimum in an ideal anti-van't Hoff−Le Bel configuration, with a germanium-centered, p_z-type LUMO, and a significantly smaller FMO gap (3.17 eV) compared to the related tetrapyrrolato germane with a tetrahedral ground state (6.76 eV, SI section 4.7). Removal of the labile thf ligands could not be achieved experimentally by prolonged exposure to high vacuum. Heating complex **1** at 80 °C under a high vacuum leads to decomposition of the sample. We reasoned that the dynamic binding would enable mirroring the peculiar nature of the anti-van't Hoff−Le Bel species.

The structural constraint enhanced Lewis acidity was pursued first by the formation of the elusive hypercoordinated germanium species. Reacting **1** with PPh_4Cl in dcm induced complete conversion to the chlorido germanate, PPh_4[CxGeCl] (**2**) (Figure 3A). SCXRD analysis of **2** verified this first example of an anionic GeN_4Cl motif (Figure S74).[13] The Ge−N distances in **2** (193.7(11)-195.0(11) pm) are slightly elongated in comparison to **1** (197.5(2) pm), and the Ge−Cl bond length (217.3(3) pm) in **2** is similar to previously known neutral Ge−Cl complexes.[14] The ^{1}H NMR spectrum of **2** showed a singlet for the pyrrole protons and a 2-fold set of signals for the ethyl group, which indicate a C_{4V} symmetry at the NMR time scale. The corresponding fluorido germanate, N^{n}Bu$_4$[CxGeF] (**3**), was prepared by the reaction with N^{n}Bu$_4$(Ph_3SiF_2) in dichloromethane and fully characterized

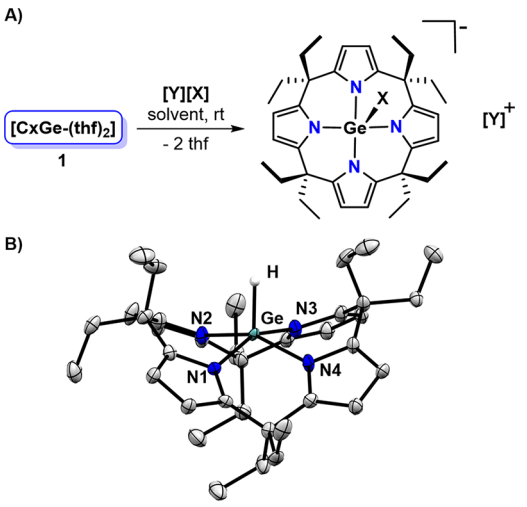

Figure 3. (A) Reactivity of **1** to form the different germanates **2**, **3**, **4**, and **5**. **2**: [Y][X] = [PPh_4][Cl], dcm, 16 h, Yield = 80%; **3**: [Y][X] = [N^{n}Bu$_4$][$SiPh_3F_2$], dcm, 10 min, Yield = 63%; **4**: [Y][X] = [NBu_4][N_3], dcm, 1 d, Yield = 82%; **5**: [Y][X] = [H][PPh_4], (1) $NaBHEt_3$, 15-Crown-5, toluene, 5 min, (2) PPh_4Cl, dcm, 4 h, Yield = 64%. (B) Solid state structure of **5**. Displacement ellipsoids are drawn at the 50% probability level. The countercation and the hydrogen atoms, except the hydride, are omitted for clarity. Selected bond lengths [pm] and angles [deg]: Ge−N1 191.2(4), N1−Ge−N3 152.6(2), and N2−Ge−N3 151.7(2).

in solution and solid state (see SI section 1.2.4). The ^{19}F NMR spectrum of **3** showed a resonance at δ = −121.3 ppm, which is significantly downfield shifted compared to neutral [(TPFC)-GeF] (δ = −156.0 ppm) or bis(Cat^{Cl})flourido-germanate (δ = −141.8 ppm) (Cat^{Cl} = perchlorocatecholato).[9a,15] We explain this downfield shift by the pronounced deshielding caused by the low-lying LUMO in the parent square-planar germane. Single crystals of **3** suitable for SCXRD could be obtained as a PPh_4[CxGeF] salt (Figure S75). The anionic N_4GeF structural motif is unknown; [(TPFC)GeF] is the only example of a related, neutral motif.[9a,13] The Ge−F (175.2(2) pm) bond distance in **3** is similar to that of [(TPFC)GeF] 173.9(15) pm.[9a] The scope of the anions was further explored by the synthesis of azido germanate, N^{n}Bu$_4$[CxGeN_3] (**4**). The ^{1}H NMR showed similar spectral features as **3**, however, broadened signals (Figure S16). Despite several attempts, single crystals of **4** suitable for SCXRD could not be obtained.

Encouraged by the stability of complexes **2**−**4**, we probed whether an anionic Ge(IV)-hydride could be realized. The reaction of **1** with $NaBHEt_3$ in toluene in the presence of 15-crown-5 resulted in the formation of sodium hydrido germanate, Na[CxGeH] (**Na-5**), which was subsequently converted to PPh_4-salt **PPh_4-5** by the reaction with PPh_4Cl (Figure 3B). Complex **5** represents, to the best of our knowledge, the first reported anionic hydrido germanate.[16] In the ^{1}H NMR spectrum of **PPh_4-5**, a resonance at δ = 7.24 ppm was observed for the germanium-bound hydride. Literature reported resonances for neutral Ge(IV) hydrides are found in the range δ = 4−6 ppm.[17] The solid-state ATR (attenuated total reflection) spectrum shows a band at $\tilde{\nu}$ = 2118 cm^{-1} corresponding to the Ge−H stretching mode (Figure S24), which is comparable to modes of neutral germanium hydrides ($\tilde{\nu}$ = 1733−2120 cm^{-1}).[17,18] These features are reminiscent of the corresponding hydridosilicate,[7b] and showcase the strong

https://doi.org/10.1021/jacs.3c04424
J. Am. Chem. Soc. 2023, 145, 17746−17754

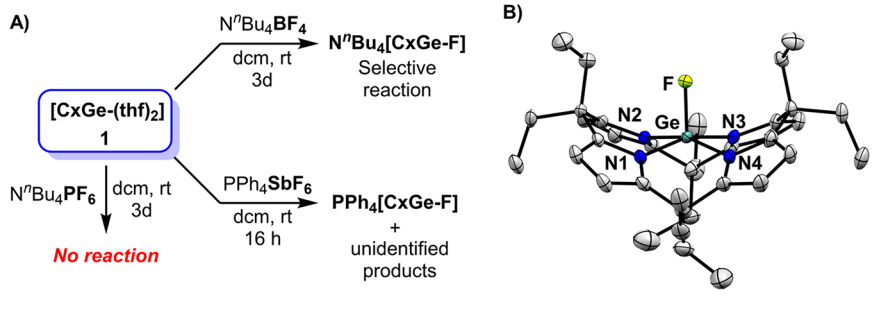

C)

Compound	FIA$_g$ (FIA$_{sol}$) [kJ mol^{-1}]
[CxGe]	445 (233)
[CxGe(thf)]	383 (160)
[CxGe(thf)$_2$] **1**	229 (69)
BF_3	338 (238)
PF_5	370 (246)
SbF_5	486 (330)

DSD-BLYP-D3(BJ)/def2-QZVPP(COSMO-RS)//r^{2}SCAN-3c

Figure 4. (A) Reactivity of **1** regarding its ability to abstract a fluoride ion of anionic fluoride adducts of the Lewis acids BF_3, PF_5, and SbF_5. (B) Solid phase structure of **3**, PPh_4 and the hydrogen atoms are omitted for clarity; thermal ellipsoids are drawn at 50% probability level. Selected bond lengths [pm] and angles [deg]: Ge−F 175.2(1), Ge−N1 193.1(2), N1−Ge−N3 161.3(8), N2−Ge−N4 161.1(8). (C) Computed FIA for gas phase FIA$_g$ and solvation corrected FIA$_{sol}$ (dcm).

electron withdrawal and bond strength from the LUMO energy lowering in the underlying square planar germane.

The most commonly used methods for the experimental quantification of *effective* Lewis acidity[19] are the Gutmann−Beckett[20] and Childs[21] method. Both methods were found unsuitable for **1**, since Et_3PO (Gutmann−Beckett) and *α,β*-unsaturated carbonyls (Childs) both react with the ligand backbone by element-ligand cooperativity (*vide infra*). Hence, the computed fluoride ion affinity (FIA) was consulted to benchmark the *global* Lewis acidity of **1**.[22] The FIA for the coordinatively saturated germanium in **1** is low (229 kJ mol^{-1}, Figure 4C). Owing to the experimentally observed lability of THF, we computed the FIA of the mono thf adduct [CxGe(thf)], yielding 383 kJ mol^{-1} (in gas phase) and 161 kJ mol^{-1} (solvent corrected) (see section 4.2 of SI for details). These, and even the values of the donor-free species (445 kJ mol^{-1}), revealed a Lewis acidity substantially below that of Lewis superacidic SbF_5 (FIA(SbF_5) = 487 kJ mol^{-1}/ FIA$_{solv}$(SbF_5) = 330 kJ mol^{-1}). Still, we decided to check the computational FIA values experimentally by competition experiments with salts of $[BF_4]^-$ (FIA(BF_3) = 338 kJ mol^{-1}/ FIA$_{solv}$(BF_3) = 238 kJ mol^{-1}), $[PF_6]^-$ (FIA(PF_5) = 370 kJ mol^{-1}/FIA$_{solv}$(PF_5) = 246 kJ mol^{-1}), and $[SbF_6]^-$ in CD_2Cl_2, and the reaction was followed by multinuclear NMR spectroscopy. In line with computations, complex **1** abstracted a F^- ion from $[BF_4^-]$ in *N^{n}Bu$_4$BF$_4$*, cleanly forming fluoride adduct **3** within 3 days (Figure 4A). Against the more stable $[PF_6^-]$, no reaction was observed even after 3 days (Figure 4A), aligning with the calculated FIA of PF_5 (Figure 4C). To our surprise, **1** reacted with the most stable $[SbF_6^-]$ within 16 h at room temperature to completion, which is even faster than for the much better fluoride ion donor $[BF_4^-]$. Analysis of NMR spectra of the reaction between **1** and $PPh_4[SbF_6]$ showed a product mixture with at least two significant species forming. One of the products was identified as PPh_4-**3**, and this was further verified by SCXRD analysis (Figure S75). Although the exact nature of a second major product could not be determined, the ^{1}H and ^{13}C{^{1}H} NMR spectra of the reaction mixture show characteristic signals of a dearomatization of the pyrrole rings and a double protonated ligand-backbone (protonation at the *α*-C of pyrrole ring, SI section 1.2.7.6). The source of protons remains unknown but indicates radical pathways initiated from oxidized intermediates of **1**. Calix[4]pyrrolato ligands are known for their ability to partake in redox processes.[6a,10,12] The tetraanionic form of the calix[4]pyrrolato ligand is readily oxidized with the simultaneous formation of a C−C bond between two adjacent pyrrole rings, referred to as Δ-form. This form is known to react further, frequently leading to ligand decomposition.[6a,10,12] Hence, we suspected the reactivity of **1** with $[SbF_6]^-$ to include a redox event, which combines the abstraction of the fluoride ion from $[SbF_6]^-$ with the oxidation of a calix[4]-pyrrolato ligand by the concomitantly formed SbF_5 (which is known to be a potent oxidant).[22a,23] Notably, it is unlikely that either step can happen independently. The FIA$_g$ values of [CxGe(thf)] and even of the parent donor-free germane are too low for fluoride abstraction from $[SbF_6]^-$ (Figure 4C). On the other hand, a reduction of $[SbF_6]^-$ by **1** should not be thermodynamically feasible, since compound **1** is not a potent reductant, showing irreversible two-electron oxidation at 0.35 V vs ferrocene/ferrocenium (Figure S81), while SbF_6^- not an oxidant.[24] Instead, we propose that the reaction proceeds by a fluoride-coupled electron transfer, reminiscent of proton-coupled electron transfer, that leads to substantial barrier lowering and thermodynamic modulation.[25]

Fluoride ion abstraction continuously increases the oxidation potential of F···SbF_5, which concomitantly oxidizes the calix[4]pyrrolato ligand. The Sb(III)F_n^{3-n} byproducts serve as fluoride ion sources that lead to the partial formation of **3**. Notably, releasing a strong oxidant (SbF_5) appears to be crucial to driving the reaction, as a similar reaction does not proceed with $[PF_6]^-$, which would form the much weaker oxidant PF_5. Although this proposal withstands a detailed analysis due to the disruptive nature of the reaction and the variety of formed products, its mere observation outlines an important aspect: a successful fluoride abstraction from $[SbF_6^-]$ does not confirm Lewis superacidity *per se* (FIA > SbF_5), since the involvement of the redox process can have a significant effect on the outcome, if the Lewis acid in question is redox-active. Hence, we recommend including the reaction with redox-innocent $[PF_6^-]$ and $[BF_4^-]$ in the experimental verification of Lewis superacidity.

In complex **1**, germanium-centered LUMO and ligand-located HOMO are suitable for cooperative bond activation. We started to investigate such reactivity with simple carbonyls. An NMR scale reaction of compound **1** with *p*-nitrobenzaldehyde resulted in an element-ligand cooperative addition of the C−O bond (Figure 5a and Figure S63). The reactivity of **1** with isopropyl alcohol was also tested, yielding complex **6**, [^{H}CxGe-O^{i}Pr] (^{H}Cx = monoprotonation at *α*-C), through O−H bond addition over Ge and *α*-carbon of the pyrrole ring (Figure 5a). Complex **6** was fully characterized in solution and the solid state (see SI). Up to this point, the structurally constrained Ge(IV) species behaves similarly to

https://doi.org/10.1021/jacs.3c04424
J. Am. Chem. Soc. 2023, 145, 17746−17754

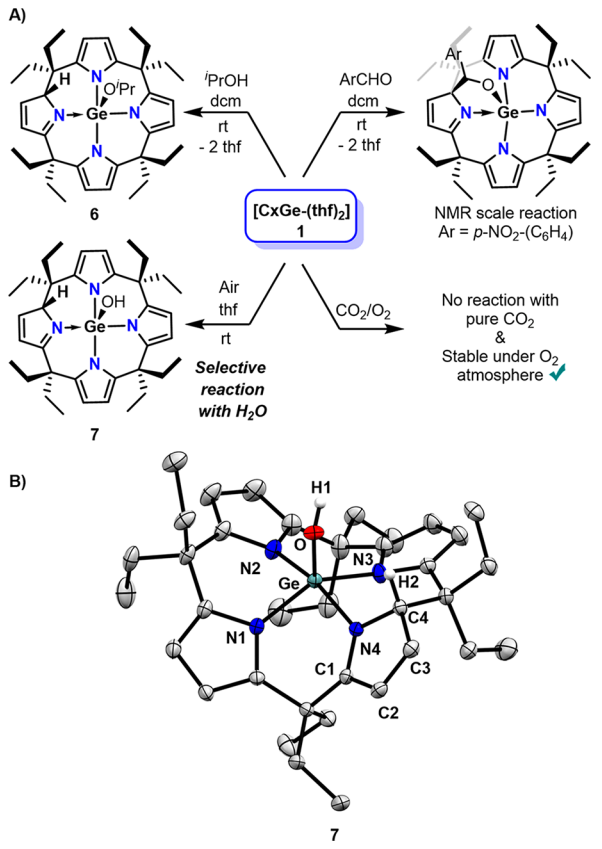

Figure 5. (A) Reactivity of **1** toward different substrates. (B) Solid phase structure of **7**. Displacement ellipsoids are drawn at 50% probability level. Hydrogen atoms, except H1 and H2, are omitted for clarity. Selected bond lengths [pm] and angles [deg]: Ge−O 176.6(1), Ge−N1 191.9(2), Ge−N4 202.4(1), N4−C1 130.4(3), C1−C2 145.9(2), C2−C3 134.4(3),C3−C4 149.5(2), N4−C4 146.0(2), N1−Ge−N3 144.5(6), N2−Ge−N4 166.2(6).

the square planar calix[4]pyrrolato aluminate anion.[26] To investigate a potential reactivity with dioxygen, as observed for the aluminate,[27] we tested the behavior of **1** toward air. To our surprise, exposing a solution of **1** in thf to air led to a selective reaction, but this time with water. The ^{1}H NMR spectrum of the reaction mixture showed characteristic signals for one dearomatized pyrrole ring (δ = 8.09 and 7.26 ppm). The reaction product was isolated as the compound [^{H}CxGe−OH] (**7**) (Figure 5a). SCXRD analysis of **7** confirmed the selective element-ligand cooperative addition of H_2O (Figure 5b). Accordingly, unlike calix[4]pyrrole aluminates or gallates, complex **1** neither reacts with dry O_2 nor with dry CO_2.[5e,27]

Following the concept of labile donors like thf to access anti-van't Hoff−Le Bel reactivity, we tried to vary the axial ligands toward stronger and weaker ends. By dissolving **1** in pyridine, the bis-pyridine adduct [CxGe-py$_2$] **1-py$_2$** was easily accessible (SI section 1.2.8). The binding enthalpy for the first pyridine from **1** to a square pyramidal germane is computed to $\Delta H_{(dcm)}$ = −19.1 kcal mol^{-1} ($\Delta G_{(dcm)}$ = −6.9 kcal mol^{-1}), thus more firmly bound compared to THF. The binding enthalpy of the second pyridine was computed to $\Delta H_{(dcm)}$ = −32.8 kcal mol^{-1} ($\Delta G_{(dcm)}$ = −20.5 kcal mol^{-1}). Accordingly, the ^{1}H NMR spectrum of **1-py$_2$** with excess pyridine shows two sets of signals corresponding to free and Ge-bound pyridine (Figure S69), which contrasts with that of **1** in the presence of excess thf, showing only one broad signal due to exchange (Figure S4). Nonetheless, the NOESY NMR spectrum of **1-py$_2$** with excess pyridine still shows exchange signals between the free and Ge-bound pyridine (Figure S71). Due to the stronger binding of the pyridine in **1-py$_2$** its reactivity is lowered. Even under harsh conditions, **1-py$_2$** does not react, e.g., with activated benzaldehydes (SI section 1.2.9).

To gauge the reactivity of the square planar compound stabilized with donors weaker than thf, the acetonitrile adduct was considered. Subjecting compound **1** toward excess CH_3CN led to forming of a new compound **8** with substantially lowered symmetry, isolable in 67% yield (Figure 6A). SCXRD analysis revealed an open chain pyrrolato germanium in distorted trigonal-bipyramidal geometry with one incorporated unit of acetonitrile (Figure 6B). One pyrrole ring is rearranged by forming a new Ge−C bond with 190.6(2) pm, in the typical range of Ge−C single bonds between 190 and 205 pm, and a proton shifted to pyrrole nitrogen.[28] The structure of **8** is also confirmed in solution by the combination of multinuclear NMR (SI section 1.2.7.3). While the configuration of the formed olefin in **8** cannot unequivocally be determined in solid-state structure due to disorder, the *Z*-isomer was observed as the major product by a NOESY correlation between the CH_3 group and pyrrolic proton (Figure S44). Thus, while aiming for an even weaker donor adduct, a new reactivity mode of the calix[4]pyrrole-p-block class toward nitriles was induced.

Interestingly, a short-lived intermediate could be observed upon reacting **1** with a small amount of acetonitrile and rapid NMR spectroscopy, which can be assigned as the primary element-ligand cooperative addition product (Figure 6C and Figures S45−S49).

We aimed to gain mechanistic insights into the reaction pathway by DFT calculations (Figure 6D). Starting from the bis-MeCN adduct [CxGe-(MeCN)$_2$], the first step involves the dissociation of one MeCN molecule and the formation of pentacoordinate [CxGe-(MeCN)]. The enhanced Lewis acidity of the pentacoordinate Ge center activates the C−N triple bond toward nucleophilic attack of the α-C atoms (C10) to form the corresponding **INT1**, observed spectroscopically (Figure 6C). With the possible driving force of reducing strain of the system, the C3−C10 single bond is elongated until C−C bond cleavage and the formation of the less strained **INT2** with a distorted square pyramidal coordination geometry follows. This is followed by a series of steps, including C(sp^3)−H (ethyl group) and C(sp^2)−H (pyrrolic CH bond) activation and the formation of two new NH bonds. Due to the multitude of different pathways coupled with the conformational flexibility of the eight ethyl groups, we could not fully elucidate these remaining steps (see section S4.3 in the SI for further discussion). However, it is shown that the overall reaction cascade from **INT2** to final product **8** is strictly downhill, overall supporting the reported reactivity. This sequence involves, to the best of our knowledge, the first spontaneous reaction of a CN triple bond by means of a structural constraint approach. Interestingly, the reaction cascade is initiated only by deliberating one of the two weakly bound acetonitriles and in line with our hypothesis to achieve reactivities within the anti-Van't Hof−Le Bel manifold by ligand lability. Compound **8** is also interesting in context of helical chirality in tetrapyrrole systems for optical polarization.[29]

https://doi.org/10.1021/jacs.3c04424
J. Am. Chem. Soc. 2023, 145, 17746−17754

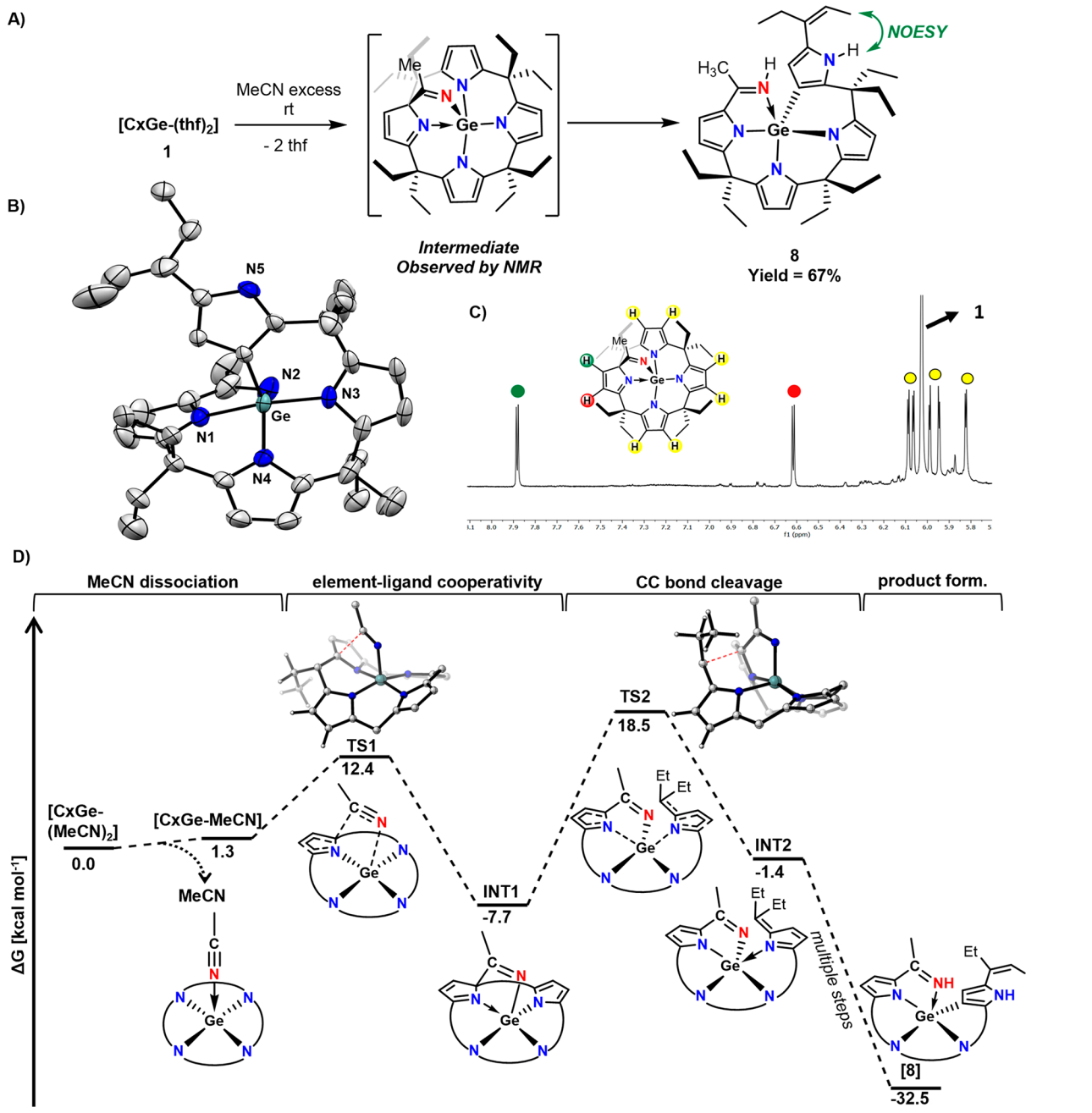

Figure 6. (A) Synthesis of **8** via 1,2-addition product as an intermediate. (B) Solid phase structure of **8**. Displacement ellipsoids are drawn at 50% probability level. Hydrogen atoms are omitted for clarity. Selected bond lengths [pm] and angles [deg]: Ge−N1 198.1(2), Ge−C6 190.6(2), N2−C8 132.7(4), N2−Ge−N4 120.6(1), N2−Ge−C8 105.3(1), N4−Ge−C6 132.1(9), and N1−Ge−N3 170.1(9). (C) Cut-out of ^{1}H NMR (600 MHz, 298 K, CD_2Cl_2) spectrum of the intermediate 1,2-addition product with assignment of the signals. (D) Reaction profile of the formation of **8** calculated at the DSD-PBEP86-D3(BJ)/def2-QZVPP+SMD(DCM)//r^{2}SCAN-3c level with possible intermediates and transition states.

CONCLUSIONS

The present work demonstrates how the reactivity of anti-Van't Hof−Le Bel germanium(IV) can be explored by ligand lability from an appropriate hydrocarbon soluble precursor obtained at a multigram scale. While the calix[4]pyrrolato macrocycle guarantees square-planarity in the donor-free germane, two weakly bound thf groups provide robustness. The precomplex exemplifies the unique behavior of non-VSEPR germanium toward different ends:

(1) New germanium adducts, including the first anionic hydrido germanate, are obtained by profiting from the LUMO energy lowering through planarization.

(2) A counterintuitive trend in experimental, global Lewis acidity is observed, which can be attributed to the redox-active nature of the calix[4]pyrrolato ligand framework. This observation should not be restricted to this specific substance class but urges caution to each experimental verification of Lewis superacidity if concomitant redox chemistry can be expected.

(3) By modulation of donor strength, the reactivity can be tuned, and diverse element-ligand cooperative bond

https://doi.org/10.1021/jacs.3c04424
J. Am. Chem. Soc. 2023, 145, 17746−17754

activation modes are leveraged by the beneficial interplay with the anti-van't Hoff–Le Bel induced Lewis acidity enhancement. With acetonitrile as the weakest donor, an unprecedented activation of a CN triple bond is disclosed, which allows attractive transformation of the calix[4]pyrrolato framework into a germanium(IV)-constricted helical structure.[29]

Overall, this study pushes the potential of structural constraint approaches to enhance the reactivity of p-block elements in their most stable oxidation states. Exploiting element-ligand cooperative substrate activation modes for catalysis and isolating alternative weak adducts are currently under investigation.

■ ASSOCIATED CONTENT

Supporting Information

The Supporting Information is available free of charge at https://pubs.acs.org/doi/10.1021/jacs.3c04424.

Experimental procedure, NMR spectra of the compounds, X-ray diffraction details and data of compounds **1**, **2**, **PPh$_4$-4**, **K-5**, **6**, **7**, **8**, **1-py$_2$**, cyclic voltammetry of **1** and DFT calculations. (PDF)

Accession Codes

CCDC 2259390–2259397 contain the supplementary crystallographic data for this paper. These data can be obtained free of charge via www.ccdc.cam.ac.uk/data_request/cif, or by emailing data_request@ccdc.cam.ac.uk, or by contacting The Cambridge Crystallographic Data Centre, 12 Union Road, Cambridge CB2 1EZ, UK; fax: +44 1223 336033.

■ AUTHOR INFORMATION

Corresponding Author

Lutz Greb − *Anorganisch-Chemisches Institut, Ruprecht-Karls-Universität Heidelberg, Heidelberg 69120, Germany;* orcid.org/0000-0002-5253-419X; Email: greb@uni-heidelberg.de

Authors

Ravi Yadav − *Anorganisch-Chemisches Institut, Ruprecht-Karls-Universität Heidelberg, Heidelberg 69120, Germany*

Paul Janßen − *Anorganisch-Chemisches Institut, Ruprecht-Karls-Universität Heidelberg, Heidelberg 69120, Germany*

Marcel Schorpp − *Anorganisch-Chemisches Institut, Ruprecht-Karls-Universität Heidelberg, Heidelberg 69120, Germany;* Present Address: Marcel Schorpp - Universität Regensburg, Regensburg 93053, Germany

Complete contact information is available at: https://pubs.acs.org/10.1021/jacs.3c04424

Author Contributions

‡R.Y. and P.J. contributed equally.

Funding

Financial support for this project was provided by the European Research Council (ERC) under the European Union's Horizon 2020 research and innovation program (grant agreement no. 948708).

Notes

The authors declare no competing financial interest.

■ ACKNOWLEDGMENTS

We thank H. Sahlmann for support. We acknowledge support by the state of Baden-Württemberg through bwHPC and the German Research Foundation (DFG) through grant no. INST 40/575-1 FUGG (JUSTUS 2 cluster).

■ REFERENCES

(1) (a) Dunn, N. L.; Ha, M.; Radosevich, A. T. Main Group Redox Catalysis: Reversible P^{III}/P^{V} Redox Cycling at a Phosphorus Platform. *J. Am. Chem. Soc.* **2012**, *134* (28), 11330−11333. (b) McCarthy, S. M.; Lin, Y.-C.; Devarajan, D.; Chang, J. W.; Yennawar, H. P.; Rioux, R. M.; Ess, D. H.; Radosevich, A. T. Intermolecular N−H Oxidative Addition of Ammonia, Alkylamines, and Arylamines to a Planar σ3-Phosphorus Compound via an Entropy-Controlled Electrophilic Mechanism. *J. Am. Chem. Soc.* **2014**, *136* (12), 4640−4650. (c) Reichl, K. D.; Dunn, N. L.; Fastuca, N. J.; Radosevich, A. T. Biphilic Organophosphorus Catalysis: Regioselective Reductive Transposition of Allylic Bromides via PIII/PV Redox Cycling. *J. Am. Chem. Soc.* **2015**, *137* (16), 5292−5295. (d) Robinson, T. P.; De Rosa, D. M.; Aldridge, S.; Goicoechea, J. M. E-H Bond Activation of Ammonia and Water by a Geometrically Constrained Phosphorus(III) Compound. *Angew. Chem., Int. Ed.* **2015**, *54* (46), 13758−63. (e) Abbenseth, J.; Goicoechea, J. M. Recent developments in the chemistry of non-trigonal pnictogen pincer compounds: from bonding to catalysis. *Chem. Sci.* **2020**, *11* (36), 9728−9740. (f) Kundu, S. Pincer-Type Ligand-Assisted Catalysis and Small-Molecule Activation by non-VSEPR Main-Group Compounds. *Chem.—Asian J.* **2020**, *15* (20), 3209−3224. (g) Lipshultz, J. M.; Li, G.; Radosevich, A. T. Main Group Redox Catalysis of Organopnictogens: Vertical Periodic Trends and Emerging Opportunities in Group 15. *J. Am. Chem. Soc.* **2021**, *143* (4), 1699−1721.

(2) (a) Power, P. P. Main-group elements as transition metals. *Nature* **2010**, *463* (7278), 171−177. (b) Chu, T.; Nikonov, G. I. Oxidative Addition and Reductive Elimination at Main-Group Element Centers. *Chem. Rev.* **2018**, *118* (7), 3608−3680.

(3) (a) Stephan, D. W.; Erker, G. Frustrated Lewis Pair Chemistry: Development and Perspectives. *Angew. Chem., Int. Ed.* **2015**, *54* (22), 6400−6441. (b) Melen, R. L. Frontiers in molecular p-block chemistry: From structure to reactivity. *Science* **2019**, *363* (6426), 479−484. (c) Greb, L.; Ebner, F.; Ginzburg, Y.; Sigmund, L. M. Element-Ligand Cooperativity with p-Block Elements. *Eur. J. Inorg. Chem.* **2020**, *2020* (32), 3030−3047. (d) Stephan, D. W. Diverse Uses of the Reaction of Frustrated Lewis Pair (FLP) with Hydrogen. *J. Am. Chem. Soc.* **2021**, *143* (48), 20002−20014.

(4) (a) Hentschel, A.; Brand, A.; Wegener, P.; Uhl, W. A Sterically Constrained Tricyclic PC3 Phosphine: Coordination Behavior and Insertion of Chalcogen Atoms into P−C Bonds. *Angew. Chem., Int. Ed.* **2018**, *57* (3), 832−835. (b) Lin, Y.-C.; Gilhula, J. C.; Radosevich, A. T. Nontrigonal constraint enhances 1,2-addition reactivity of phosphazenes. *Chem. Sci.* **2018**, *9* (18), 4338−4347. (c) Gilhula, J. C.; Radosevich, A. T. Tetragonal phosphorus(v) cations as tunable and robust catalytic Lewis acids. *Chem. Sci.* **2019**, *10* (30), 7177−7182. (d) Marczenko, K. M.; Zurakowski, J. A.; Kindervater, M. B.; Jee, S.; Hynes, T.; Roberts, N.; Park, S.; Werner-Zwanziger, U.; Lumsden, M.; Langelaan, D. N.; Chitnis, S. S. Periodicity in Structure, Bonding, and Reactivity for p-Block Complexes of a Geometry Constraining Triamide Ligand. *Chem.—Eur. J.* **2019**, *25* (71), 16414−16424. (e) Tanaka, D.; Kadonaga, Y.; Manabe, Y.; Fukase, K.; Sasaya, S.; Maruyama, H.; Nishimura, S.; Yanagihara, M.; Konishi, A.; Yasuda, M. Synthesis of Cage-Shaped Aluminum Aryloxides: Efficient Lewis Acid Catalyst for Stereoselective Glycosylation Driven by Flexible Shift of Four- to Five-Coordination. *J. Am. Chem. Soc.* **2019**, *141* (44), 17466−17471. (f) Janes, T.; Diskin-Posner, Y.; Milstein, D. Synthesis and Reactivity of Cationic Boron Complexes Distorted by Pyridine-based Pincer Ligands: Isolation of a Photochemical Hofmann-Martius-type Intermediate. *Angew. Chem., Int. Ed.* **2020**, *59* (12), 4932−4936. (g) Abbenseth, J.; Townrow, O. P. E.; Goicoechea, J. M. Thermoneutral N−H Bond Activation of Ammonia

by a Geometrically Constrained Phosphine. *Angew. Chem., Int. Ed.* **2021**, *60* (44), 23625−23629. (h) Osi, A.; Mahaut, D.; Tumanov, N.; Fusaro, L.; Wouters, J.; Champagne, B.; Chardon, A.; Berionni, G. Taming the Lewis Superacidity of Non-Planar Boranes: C-H Bond Activation and Non-Classical Binding Modes at Boron. *Angew. Chem., Int. Ed.* **2022**, *61* (7), No. e202112342. (i) Volodarsky, S.; Bawari, D.; Dobrovetsky, R. Dual Reactivity of a Geometrically Constrained Phosphenium Cation. *Angew. Chem., Int. Ed.* **2022**, *61* (36), No. e202208401.

(5) (a) Myers, T. W.; Berben, L. A. Aluminum−Ligand Cooperative N−H Bond Activation and an Example of Dehydrogenative Coupling. *J. Am. Chem. Soc.* **2013**, *135* (27), 9988−9990. (b) Thompson, E. J.; Myers, T. W.; Berben, L. A. Synthesis of Square-Planar Aluminum-(III) Complexes. *Angew. Chem., Int. Ed.* **2014**, *53* (51), 14132−14134. (c) Ebner, F.; Wadepohl, H.; Greb, L. Calix[4]pyrrole Aluminate: A Planar Tetracoordinate Aluminum(III) Anion and Its Unusual Lewis Acidity. *J. Am. Chem. Soc.* **2019**, *141* (45), 18009−18012. (d) Bass, T. M.; Carr, C. R.; Sherbow, T. J.; Fettinger, J. C.; Berben, L. A. Syntheses of Square Planar Gallium Complexes and a Proton NMR Correlation Probing Metalloaromaticity. *Inorg. Chem.* **2020**, *59* (18), 13517−13523. (e) Ebner, F.; Sigmund, L. M.; Greb, L. Metal−Ligand Cooperativity of the Calix[4]pyrrolato Aluminate: Triggerable C−C Bond Formation and Rate Control in Catalysis. *Angew. Chem., Int. Ed.* **2020**, *59* (39), 17118−17124. (f) Sigmund, L. M.; Ehlert, C.; Enders, M.; Graf, J.; Gryn'Ova, G.; Greb, L. Dioxygen Activation and Pyrrole α-Cleavage with Calix[4]pyrrolato Aluminates: Enzyme Model by Structural Constraint. *Angew. Chem., Int. Ed.* **2021**, *60* (28), 15632−15640. (g) Schön, F.; Sigmund, L. M.; Schneider, F.; Hartmann, D.; Wiebe, M. A.; Manners, I.; Greb, L. Calix[4]pyrrolato Aluminate Catalyzes the Dehydrocoupling of Phenylphosphine Borane to High Molar Weight Polymers. *Angew. Chem., Int. Ed.* **2022**, *61* (22), No. e202202176. (h) Shaves, C. L.; Villegas-Escobar, N.; Clark, E. R.; Riddlestone, I. M. Diverse Cooperative Reactivity at a Square Planar Aluminium Complex and Catalytic Reduction of CO_2. *Chem.—Eur. J.* **2023**, *29* (16), No. e202203806. (i) Sigmund, L. M.; Engels, E.; Richert, N.; Greb, L. Calix[4]pyrrolato gallate: square planar-coordinated gallium(iii) and its metal−ligand cooperative reactivity with CO_2 and alcohols. *Chem. Sci.* **2022**, *13* (37), 11215−11220. (j) Volodarsky, S.; Malahov, I.; Bawari, D.; Diab, M.; Malik, N.; Tumanskii, B.; Dobrovetsky, R. Geometrically constrained square pyramidal phosphoranide. *Chem. Sci.* **2022**, *13* (20), 5957−5963. (k) Ben Saida, A.; Chardon, A.; Osi, A.; Tumanov, N.; Wouters, J.; Adjieufack, A. I.; Champagne, B.; Berionni, G. Pushing the Lewis Acidity Boundaries of Boron Compounds With Non-Planar Triarylboranes Derived from Triptycenes. *Angew. Chem., Int. Ed.* **2019**, *58* (47), 16889−16893.

(6) (a) Schorpp, M.; Yadav, R.; Roth, D.; Greb, L. Calix[4]pyrrolato Stibenium: Lewis Superacidity by Antimony(III)-Antimony(V) Electromerism. *Angew. Chem., Int. Ed.* **2022**, *61* (39), No. e202207963. (b) Li, G.; Qin, Z.; Radosevich, A. T. P(III)/P(V)-Catalyzed Methylamination of Arylboronic Acids and Esters: Reductive C−N Coupling with Nitromethane as a Methylamine Surrogate. *J. Am. Chem. Soc.* **2020**, *142* (38), 16205−16210. (c) Lim, S.; Radosevich, A. T. Round-Trip Oxidative Addition, Ligand Metathesis, and Reductive Elimination in a P^{III}/P^{V} Synthetic Cycle. *J. Am. Chem. Soc.* **2020**, *142* (38), 16188−16193. (d) Lipshultz, J. M.; Fu, Y.; Liu, P.; Radosevich, A. T. Organophosphorus-catalyzed relay oxidation of H-Bpin: electrophilic C−H borylation of heteroarenes. *Chem. Sci.* **2021**, *12* (3), 1031−1037. (e) Volodarsky, S.; Malahov, I.; Bawari, D.; Diab, M.; Malik, N.; Tumanskii, B.; Dobrovetsky, R. Geometrically Constrained Square Pyramidal Phosphoranide. *Chem. Sci.* **2022**, *13*, 5957−5963. (f) Karnbrock, S. B. H.; Golz, C.; Mata, R. A.; Alcarazo, M. Ligand-Enabled Disproportionation of 1,2-Diphenylhydrazine at a P(V)-Center. *Angew. Chem., Int. Ed.* **2022**, *61* (35), No. e202207450.

(7) (a) Ghana, P.; Rump, J.; Schnakenburg, G.; Arz, M. I.; Filippou, A. C. Planar Tetracoordinated Silicon (ptSi): Room-Temperature Stable Compounds Containing Anti-van't Hoff/Le Bel Silicon. *J. Am. Chem. Soc.* **2021**, *143* (1), 420−432. (b) Ebner, F.; Greb, L. Calix[4]pyrrole Hydridosilicate: The Elusive Planar Tetracoordinate Silicon Imparts Striking Stability to Its Anionic Silicon Hydride. *J. Am. Chem. Soc.* **2018**, *140* (50), 17409−17412. (c) Ebner, F.; Greb, L. An isolable, crystalline complex of square-planar silicon(IV). *Chem.* **2021**, *7* (8), 2151−2159. (d) Tretiakov, S.; Witteman, L.; Lutz, M.; Moret, M.-E. Strain-Modulated Reactivity: An Acidic Silane. *Angew. Chem., Int. Ed.* **2021**, *60* (17), 9618−9626.

(8) (a) Sigmund, L. M.; Maier, R.; Greb, L. The inversion of tetrahedral p-block element compounds: general trends and the relation to the second-order Jahn−Teller effect. *Chem. Sci.* **2022**, *13* (2), 510−521. (b) Sigmund, L. M.; Ehlert, C.; Gryn'ova, G.; Greb, L. Stereoinversion of tetrahedral p-block element hydrides. *J. Chem. Phys.* **2022**, *156* (19), 194113.

(9) (a) Fang, H.; Jing, H.; Zhang, A.; Ge, H.; Yao, Z.; Brothers, P. J.; Fu, X. Synthesis, Electronic Structure, and Reactivity Studies of a 4-Coordinate Square Planar Germanium(IV) Cation. *J. Am. Chem. Soc.* **2016**, *138* (24), 7705−7710. (b) Jing, H.; Ge, H.; Li, C.; Jin, Y.; Wang, Z.; Du, C.; Fu, X.; Fang, H. C−H and C−N Bond Activation of Tertiary Amines by Cationic Germanium(IV) Corrole. *Organometallics* **2019**, *38* (12), 2412−2416.

(10) Ruppert, H.; Sigmund, L. M.; Greb, L. Calix[4]pyrroles as ligands: recent progress with a focus on the emerging p-block element chemistry. *Chem. Commun.* **2021**, *57* (89), 11751−11763.

(11) These values were obtained with the PorphyStruc tool. See: Krumsieck, J.; Bröring, M. *Chem.—Eur. J.* **2021**, *27*, 11580−11588.

(12) (a) Bachmann, J.; Nocera, D. G. Multielectron Chemistry of Zinc Porphyrinogen: A Ligand-Based Platform for Two-Electron Mixed Valency. *J. Am. Chem. Soc.* **2004**, *126* (9), 2829−2837. (b) Bachmann, J.; Nocera, D. G. Multielectron Redox Chemistry of Iron Porphyrinogens. *J. Am. Chem. Soc.* **2005**, *127* (13), 4730−4743. (c) De Angelis, S.; Solari, E.; Floriani, C.; Chiesi-Villa, A.; Rizzoli, C. Oxidation of Metal-meso-Octaethylporphyrinogen Complexes Leading to Novel Oxidized Forms of Porphyrinogen Other than Porphyrins. 1. The Redox Chemistry of Nickel(II)- and Copper-(II)-meso-Octaethylporphyrinogen Complexes Occurring with the Formation and Cleavage of a Cyclopropane Unit. *J. Am. Chem. Soc.* **1994**, *116* (13), 5691−5701.

(13) Groom, C. R.; Bruno, I. J.; Lightfoot, M. P.; Ward, S. C. The Cambridge Structural Database. *Acta Crystallogr., Sect. B* **2016**, *72* (2), 171−179.

(14) (a) Komissarov, E. A.; Korlyukov, A. A.; Kramarova, E. P.; Bylikin, S. Y.; Negrebetsky, V. V.; Baukov, Y. I. Chloridobis[(2-oxoazocan-1-yl)methyl]germanium(IV) trifluoromethanesulfonate. *Acta Crystallogr., Sect. C* **2007**, *63* (4), m144−m146. (b) Henry, A. T.; Cosby, T. P. L.; Boyle, P. D.; Baines, K. M. Selective dimerization of α-methylstyrene by tunable bis(catecholato)germane Lewis acid catalysts. *Dalton Trans.* **2021**, *50* (43), 15906−15913.

(15) Roth, D.; Wadepohl, H.; Greb, L. Bis(perchlorocatecholato)-germane: Hard and Soft Lewis Superacid with Unlimited Water Stability. *Angew. Chem., Int. Ed.* **2020**, *59* (47), 20930−20934.

(16) Chen, K.-H.; Liu, Y.-H.; Chiu, C.-W. A Non-innocent Ligand Supported Germylene and Its Diverse Reactions. *Organometallics* **2020**, *39* (24), 4645−4650.

(17) Richards, A. F.; Phillips, A. D.; Olmstead, M. M.; Power, P. P. Isomeric Forms of Divalent Heavier Group 14 Element Hydrides: Characterization of Ar'(H)GeGe(H)Ar' and Ar'$(H)_2$GeGeAr'·PMe_3 (Ar' = C_6H_3-2,6-$Dipp_2$; Dipp = C_6H_3-2,6-Pri_2). *J. Am. Chem. Soc.* **2003**, *125* (11), 3204−3205.

(18) (a) Spikes, G. H.; Fettinger, J. C.; Power, P. P. Facile Activation of Dihydrogen by an Unsaturated Heavier Main Group Compound. *J. Am. Chem. Soc.* **2005**, *127* (35), 12232−12233. (b) Al-Rafia, S. M. I.; Malcolm, A. C.; McDonald, R.; Ferguson, M. J.; Rivard, E. Trapping the Parent Inorganic Ethylenes H_2SiGeH_2 and H_2SiSnH_2 in the Form of Stable Adducts at Ambient Temperature. *Angew. Chem., Int. Ed.* **2011**, *50* (36), 8354−8357. (c) Khan, S.; Samuel, P. P.; Michel, R.; Dieterich, J. M.; Mata, R. A.; Demers, J.-P.; Lange, A.; Roesky, H. W.; Stalke, D. Monomeric Sn(ii) and Ge(ii) hydrides supported by a tridentate pincer-based ligand. *Chem. Commun.* **2012**, *48* (40), 4890−4892. (d) Pineda, L. W.; Jancik, V.; Starke, K.; Oswald, R. B.; Roesky,

https://doi.org/10.1021/jacs.3c04424
J. Am. Chem. Soc. 2023, 145, 17746−17754

H. W. Stable Monomeric Germanium(II) and Tin(II) Compounds with Terminal Hydrides. *Angew. Chem., Int. Ed.* **2006**, *45* (16), 2602−2605.
(19) Erdmann, P.; Greb, L. What Distinguishes the Strength and the Effect of a Lewis Acid: Analysis of the Gutmann-Beckett Method. *Angew. Chem., Int. Ed.* **2022**, *61* (4), No. e202114550.
(20) (a) Mayer, U.; Gutmann, V.; Gerger, W. The acceptor number — A quantitative empirical parameter for the electrophilic properties of solvents. *Monatsh. Chem.* **1975**, *106* (6), 1235−1257. (b) Beckett, M. A.; Strickland, G. C.; Holland, J. R.; Sukumar Varma, K. A convenient n.m.r. method for the measurement of Lewis acidity at boron centres: correlation of reaction rates of Lewis acid initiated epoxide polymerizations with Lewis acidity. *Polymer* **1996**, *37* (20), 4629−4631.
(21) Childs, R. F.; Mulholland, D. L.; Nixon, A. Lewis acid addticts of α,β-unsaturated carbonyl and nitrile compounds. A calorimetric study. *Can. J. Chem.* **1982**, *60* (6), 809−812.
(22) (a) Greb, L. Lewis Superacids: Classifications, Candidates, and Applications. *Chem.—Eur. J.* **2018**, *24* (68), 17881−17896. (b) Erdmann, P.; Leitner, J.; Schwarz, J.; Greb, L. An Extensive Set of Accurate Fluoride Ion Affinities for p-Block Element Lewis Acids and Basic Design Principles for Strong Fluoride Ion Acceptors. *ChemPhysChem* **2020**, *21* (10), 987−994.
(23) Olah, G. A. Superacid Systems. *Superacid Chemistry*; Wiley-Backwell: Oxford, 2009; pp 35−82.
(24) Ponikvar, M.; Liebman, J. F.; Jenkins, H. D. B. The Redox Chemistry of SbF6− Ion. *Eur. J. Inorg. Chem.* **2004**, *2004* (16), 3273−3276.
(25) (a) Weinberg, D. R.; Gagliardi, C. J.; Hull, J. F.; Murphy, C. F.; Kent, C. A.; Westlake, B. C.; Paul, A.; Ess, D. H.; McCafferty, D. G.; Meyer, T. J. Proton-Coupled Electron Transfer. *Chem. Rev.* **2012**, *112* (7), 4016−4093. (b) Tyburski, R.; Liu, T.; Glover, S. D.; Hammarström, L. Proton-Coupled Electron Transfer Guidelines, Fair and Square. *J. Am. Chem. Soc.* **2021**, *143* (2), 560−576.
(26) (a) Ebner, F.; Sigmund, L. M.; Greb, L. Metal-Ligand Cooperativity of the Calix[4]pyrrolato Aluminate: Triggerable C-C Bond Formation and Rate Control in Catalysis. *Angew. Chem., Int. Ed.* **2020**, *59* (39), 17118−17124. (b) Sigmund, L. M.; Greb, L. Reversible OH-bond activation and amphoterism by metal-ligand cooperativity of calix[4]pyrrolato aluminate. *Chem. Sci.* **2020**, *11* (35), 9611−9616.
(27) Sigmund, L. M.; Ehlert, C.; Enders, M.; Graf, J.; Gryn'ova, G.; Greb, L. Dioxygen Activation and Pyrrole alpha-Cleavage with Calix[4]pyrrolato Aluminates: Enzyme Model by Structural Constraint. *Angew. Chem., Int. Ed.* **2021**, *60* (28), 15632−15640.
(28) Baines, K. M.; Stibbs, W. G. The molecular structure of organogermanium compounds. *Coord. Chem. Rev.* **1995**, *145*, 157−200.
(29) Urban, A. J.; Yamamoto, H. M. Strong and Tunable Near-Infrared Circular Dichroism in Helical Tetrapyrrole Complexes. *Chem.—Eur. J.* **2023**, No. e202300940.

https://doi.org/10.1021/jacs.3c04424
J. Am. Chem. Soc. 2023, 145, 17746−17754